Science Advances
AAAS

advances.sciencemag.org/cgi/content/full/5/10/eaaw5537/DC1

Supplementary Materials for

Pioneer interneurons instruct bilaterality in the Drosophila olfactory sensory map

Rashmit Kaur, Michael Surala, Sebastian Hoger, Nicole Grössmann, Alexandra Grimm, Lorin Timaeus, Wolfgang Kallina, Thomas Hummel*

*Corresponding author. Email: thomas.hummel@univie.ac.at

Published 23 October 2019, *Sci. Adv.* **5**, eaaw5537 (2019)
DOI: 10.1126/sciadv.aaw5537

This PDF file includes:

Fig. S1. Unilateral versus bilateral olfactory circuit organization within Diptera.
Fig. S2. Comprehensive analysis of unilateral and bilateral projecting antennal ORN axon in *Neuroglian* mutant (see also table in Fig. 1).
Fig. S3. Neuroglian expression during development.
Fig. S4. Neuroglian expression in midline glia cells is dispensable for bilateral ORN connectivity.
Fig. S5. Cell-specific loss of Neuroglian in cPINs affects bilateral olfactory map formation.
Fig. S6. Ablation of cPINs affects bilateral connectivity of ORNs.
Fig. S7. cPINs segregate from PNs in early AL development.
Fig. S8. Cell autonomous and non-autonomous function of Neuroglian in cPINs and ORNs.
Fig. S9. Neuroglian affects olfactory commissure development of CSD neurons.
Table S1. Genotype of experiments.
Reference (*49*)

Supplementary Materials

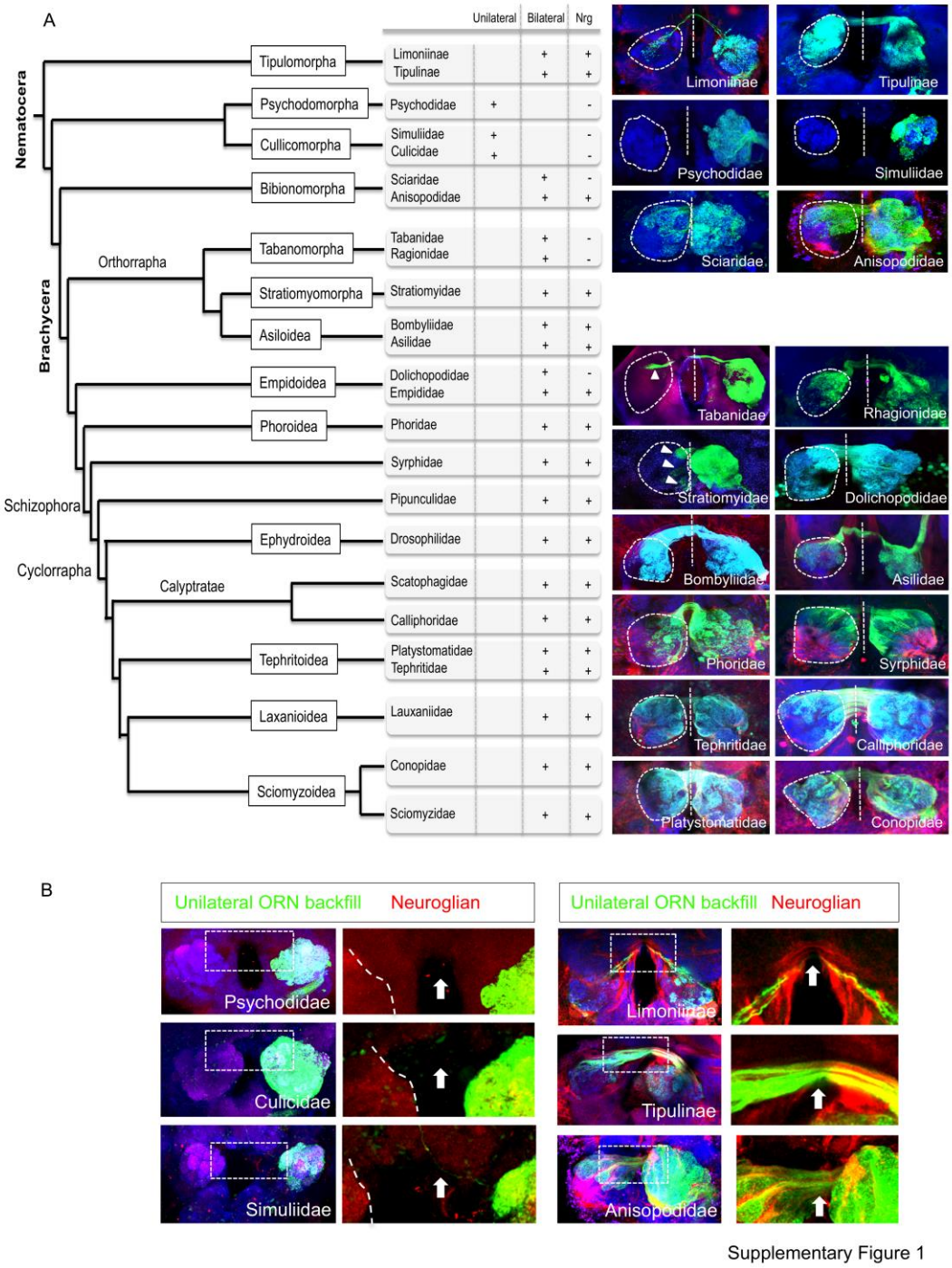

Supplementary Figure 1

Fig. S1. Unilateral versus bilateral olfactory circuit organization within Diptera. (**A**) Phylogenetic tree of Diptera consisting of the two suborders Nematocera and Brachycera, adopted from (*49*). Following unilateral antennal nerve labeling backfills (right antenna) of 1-2 representative species for each of the analyzed 26 families, the contralateral AL innervation (dotted circle) was determined and classified into unilateral (no labeling), weak (white arrowhead) and strong bilateral

innervation. Within Nematocera, a dynamic organization of uni- and bilateral olfactory map can be observed. In basal Brachycera ("Orthorrhapha"), the bilateral innervation of sensory neurons becomes more prominent and strong bilateral maps are found in all analyzed Schizophora species. (**B**) Neuroglian (Nrg) expression at the dorsal antennal lobe midline. In Nematocera species with a unilateral ORN innervation, no Nrg positive midline commissures can be detected. In contrast, Nematocera and basal Brachycera species with bilateral ORN innervation show strong Nrg expression of the olfactory commissure. Labeling: Anterograde backfill by neurobiotin (green) visualized by Avidin-Alexa Fluor488, neuropil marker DN-Cadherin (blue), anti BP104 staining shows neuronal specific isoform of Nrg (red).

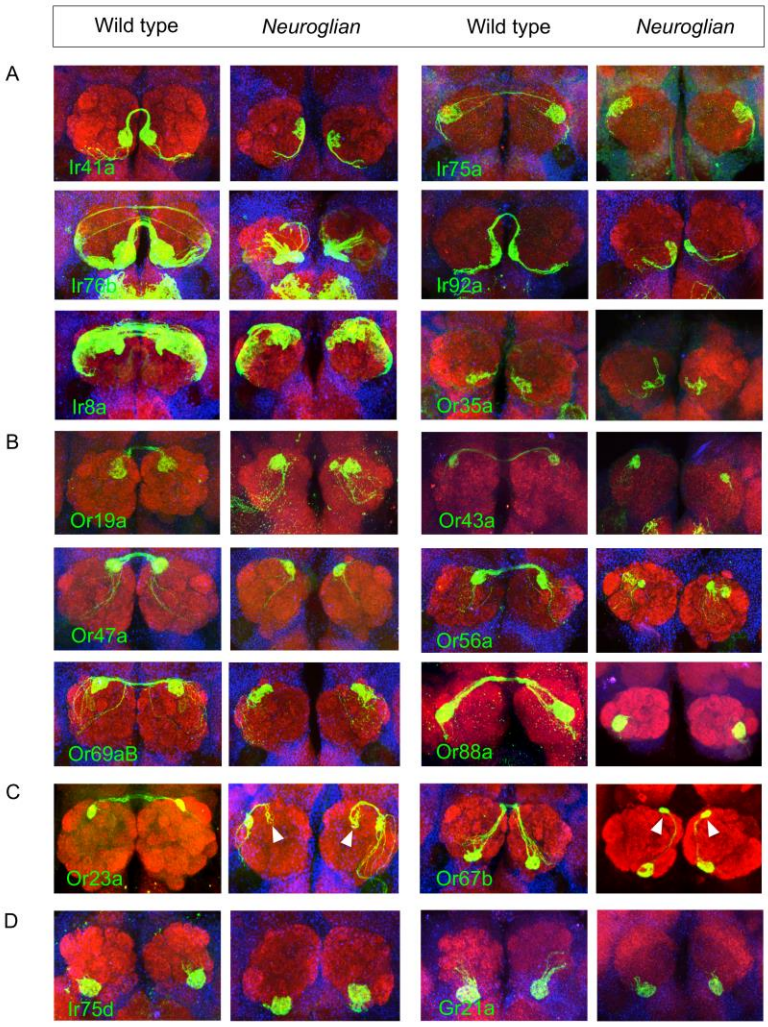

Supplementary Figure 2

Fig. S2. Comprehensive analysis of unilateral and bilateral projecting antennal ORN axon in *Neuroglian* mutant (see also table in Fig. 1). (**A**-**D**) Bilateral olfactory map is disrupted in *Nrg* mutant: (A) ORN class specific analysis of bilateral *atonal*-positive pioneer ORNs in wild type and *Nrg* mutant. In the wild type AL, ORN axons converge tightly onto their specific glomeruli. In *Nrg* mutants, the commissural tract is lost in all six ORN classes and axons innervate their cognate ipsilateral target. (B, C) Analysis of bilateral *amos*-positive follower ORNs in wild type and *Nrg* mutant. Like pioneers, wild type follower ORN axons innervate their respective ipsi- and contralateral glomerulus in the mirror symmetric AL. In *Nrg*

mutants, most bilateral ORN classes precisely target the ipsilateral glomerulus. In a small subset of *Nrg* mutant ORN classes (Or23a, Or67b), axons occasionally overshoot their ipsilateral target glomerulus and terminate at the dorsal midline (arrowheads in C). (D) Unilateral projecting *atonal* and *amos* ORN classes are unaffected in *Nrg* mutant. Genotypes: Wild type: *nrg^{849}/+;UAS-mCD8::GFP;Ir/Or-Gal4* (on II or III) *or nrg^{849}/+;Or-mCD8::GFP;* (on II or III). *Nrg* mutant: *nrg^{849}/y;UAS-mCD8::GFP; Ir/Or-Gal4* (on II or III) *or nrg^{849}/y;Or-mCD8::GFP;* (on II or III), except for Ir75d which was visualized using *R80H12-Gal4.* Labeling: All ORN axons are labeled by Or specific Gal4 driven UAS-mCD8::GFP or reporter lines which were stained with anti-GFP (in green), counterstained with neuropil marker DN-cadherin (red) and cell bodies are visualized with TOTO-3 (blue).

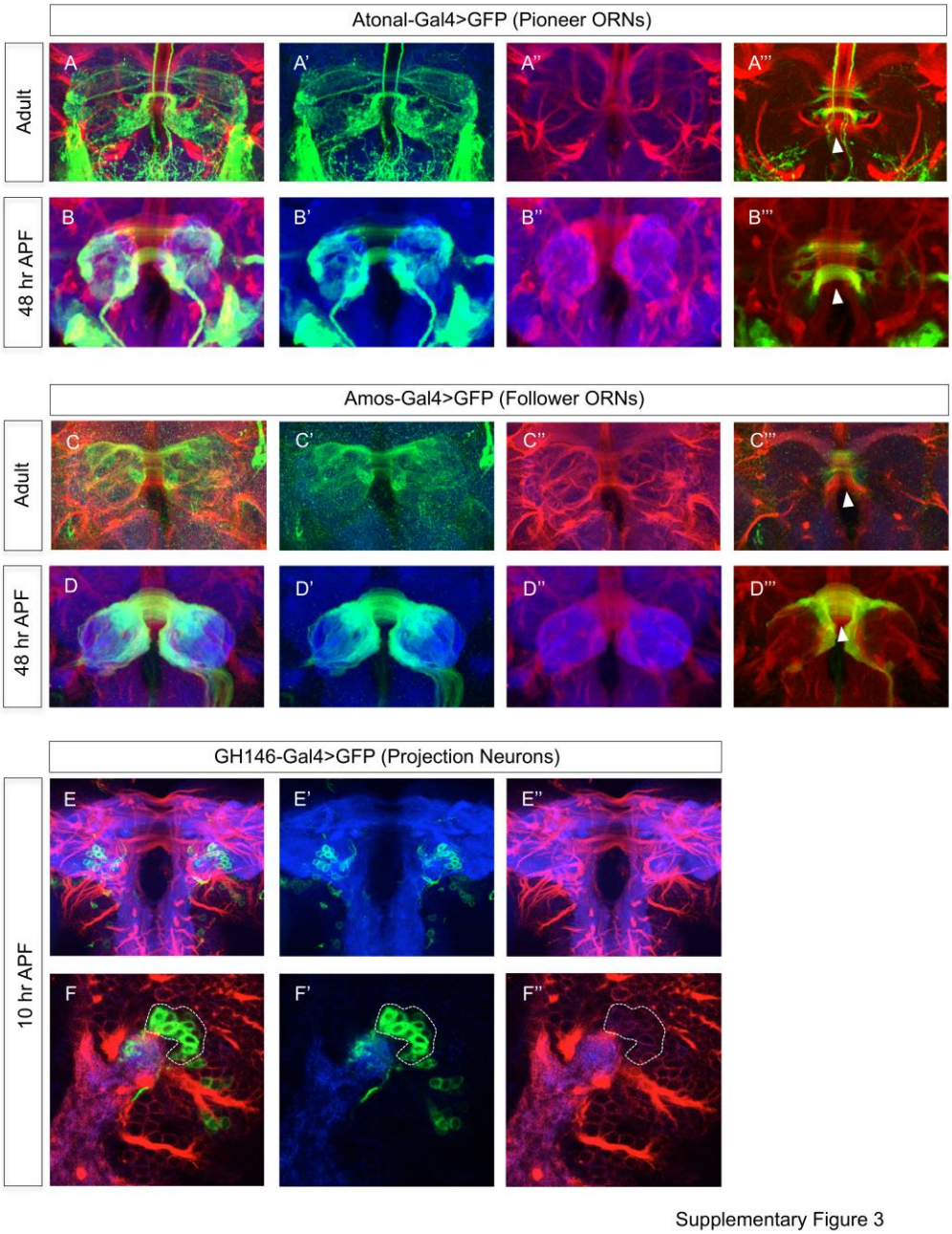

Fig. S3. Neuroglian expression during development. (**A-F**) During pupal development Nrg displays differential expression in the olfactory system. Analysis of Nrg expression in axons of *atonal*-positive pioneer ORNs (A, B), and *amos*-positive follower ORNs (C, D). Nrg (red) is strongly enriched on all the pioneer and follower ORN axons (green) during adult (A and C) and pupa (B and D) respectively. Nrg expression is seen on tightly fasciculated olfactory commissure fibers (few posterior Z- projections) in adult and pupa (white arrow head in A'''- D'''). (E-F) In early pupal development, strong Nrg expression can be observed in most commissural fibers (E) and a weak expression on unilateral projection neurons (F, cell bodies in

white circle). Genotypes: (A-B’’’) *;UAS-mCD8::GFP;atonal-Gal4;* (C-D’’’) *;amos-Gal4;UAS-mCD8::GFP;* (E-F’’’) *;UAS-mCD8::GFP;GH146-Gal4;*. Labeling: All neuronal axons are labeled by Gal4 driven UAS-mCD8::GFP which were stained with anti-GFP (in green), counterstained with neuropil marker DN-cadherin (blue) and anti BP104 staining shows neuronal specific isoform of Nrg (red).

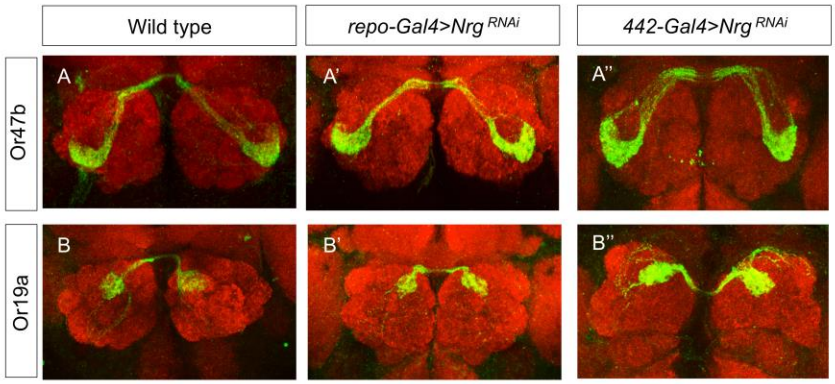

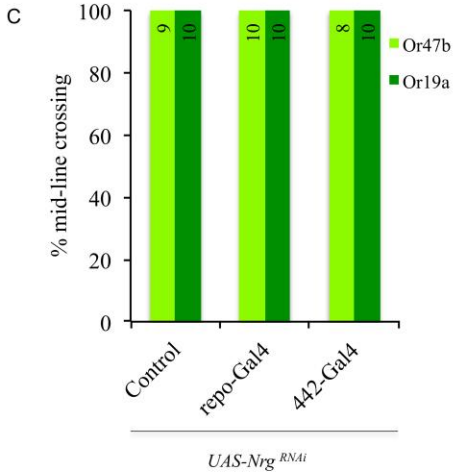

Supplementary Figure 4

Fig. S4. Neuroglian expression in midline glia cells is dispensable for bilateral ORN connectivity. (**A**-**B’’**) Targeted Nrg RNAi in two different glia populations (*repo-Gal4 and 442-Gal4*) did not affect the bilateral connectivity (A’, A’’, B’, B’’) and the innervation pattern of ORN classes as compared to wild type (A, B). (C) Quantification of bilateral connectivity of the analyzed ORN classes. Genotypes: (A, B) *;UAS-Nrg^{RNAi};Or-mCD8::GFP/+* (A’, B’) *;UAS-Nrg^{RNAi};Or-mCD8::GFP/repo-Gal4* (A’’, B’’) *;UAS-Nrg^{RNAi};Or-mCD8::GFP/442-Gal4*. Labeling: All neuronal axons are labeled by Or-mCD8::GFP reporter which were stained with anti-GFP (in green), counterstained with neuropil marker DN-cadherin (red).

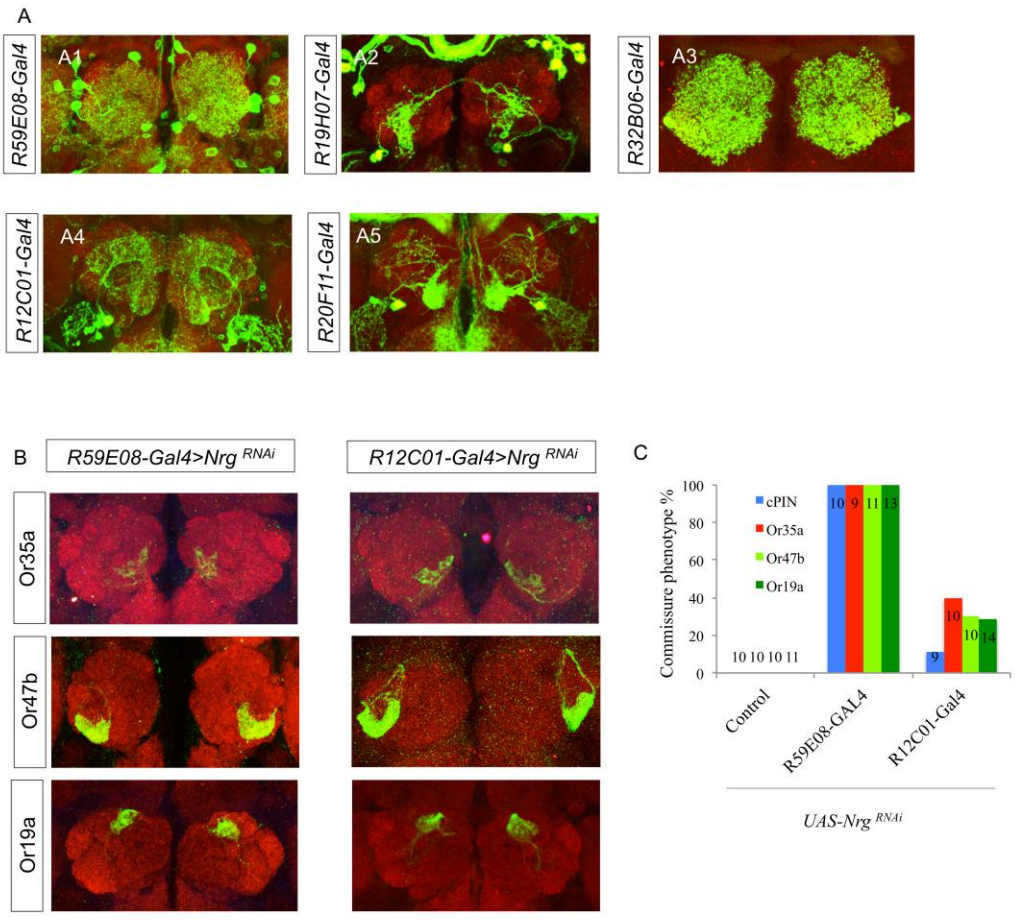

Supplementary Figure 5

Fig. S5. Cell-specific loss of Neuroglian in cPINs affects bilateral olfactory map formation. (**A**) Expression pattern of five identified Gal4 driver lines which lead to a UAS-RNAi phenotype in bilateral ORNs. These Gal4 lines were divided, based on the penetrance of the ORN connectivity phenotype, into two groups, strong (A1-A3) and weak (A4-A5). Gal4 lines A1 and A3 showed variable expression pattern, labeling cells from both ventro-lateral and lateral clusters during the development (data not shown). (**B**) Example of ORN connectivity phenotypes in a strong (*R59E08-Gal4*) and a weak (*R12C01-Gal4*) driver line for pioneer (Or35a) and follower ORNs (Or47b and Or19a).

(**C**) Quantification of commissural phenotypes observed in cPINs and ORNs upon Nrg knockdown in cPINs. Genotypes: (A1-A5) *;UAS-mCD8::GFP;Rubin-Gal4;*. (B) *;UAS-Nrg^{RNAi};Or-mCD8::GFP/Rubin-Gal4* (C) For cPINs - *;UAS-mCD8::GFP/UAS-Nrg^{RNAi};Rubin-Gal4.* For ORNs - same as B. Labeling: (A1-A5) cPINs are labeled by Gal4 driven UAS-mCD8::GFP which were stained with anti-GFP (in green), counterstained with neuropil marker DN-cadherin (red). (B) ORN axons are labeled by Or reporter lines, which were stained with anti-GFP (in green), counterstained with neuropil marker DN-cadherin (red).

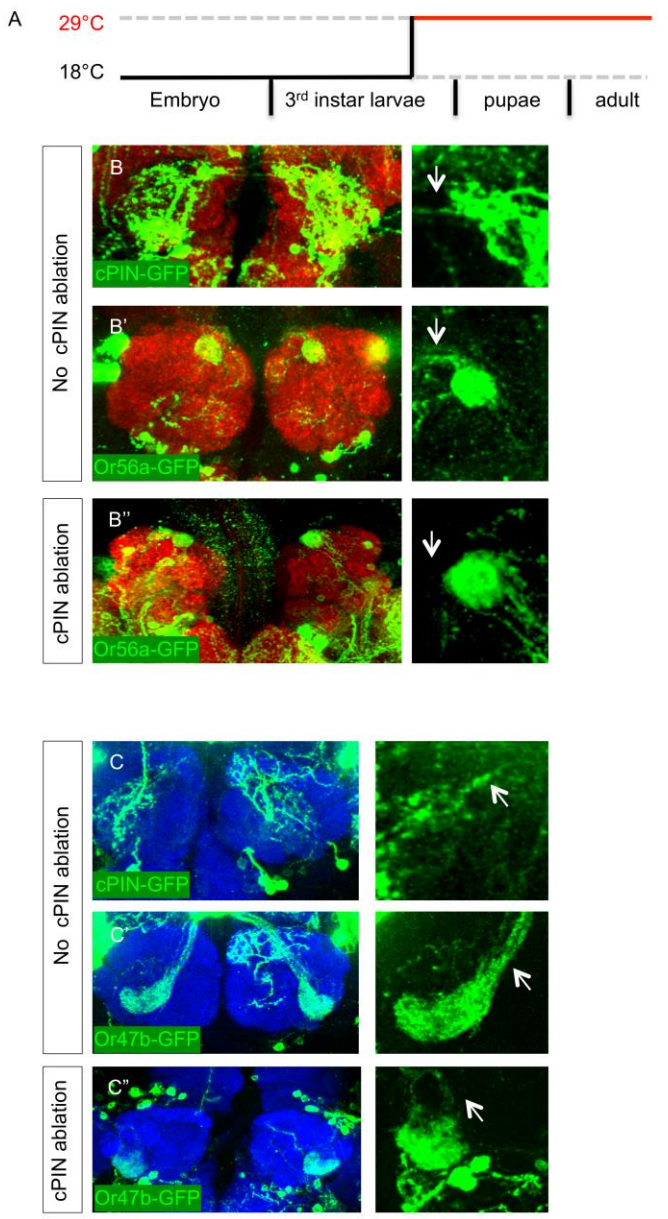

Supplementary Figure 6

Fig. S6. Ablation of cPINs affects bilateral connectivity of ORNs. (**A**) Schematic illustrating the time point of temperature shift experiments (red line). (**B-C**) Two different transgenes lines were used to perform cPINs ablation. Either, UAS-hid or UAS-DTI were expressed in cPINs from late 3rd instar larval stage onwards under the control of Gal4 as indicated in A. In those cases where targeted expression of UAS-hid did not result in cPIN ablation, the adult brains displayed wild type like morphology (B). In such cases, ORNs showed bilateral innervation (B'). cPIN and ORN commissures are indicated by white arrow in the inset. In cases where cPINs were either full ablated or strongly reduced,

bilateral ORNs fail to project contralaterally (B”). Loss of ORN commissure is indicated by white arrow in the inset. Expression of UAS-DTI also showed two connectivity phenotypes: wild type cPIN together with bilateral ORNs (C and C’) or loss of cPINs combined with unilateral ORN targeting (C”)**.** Genotypes: (B) *;R19H07-LexA, LexAop2-mGFP/Or56a-mCD8::GFP;R19H07-Gal4/UAS-hid,Gal80^{ts}* (C) *;R19H07-LexA, LexAop2-mGFP/UAS-DTI; Or47b-mCD8::GFP/R19H07-Gal4*. Labeling: All the cPIN neurites are labeled by LexA driven LexAop2-mGFP, and ORN axons are labeled by Or-mCD8::GFP reporter which were stained with anti-GFP (in green), counterstained with neuropil marker DN-cadherin (red in B and blue in C).

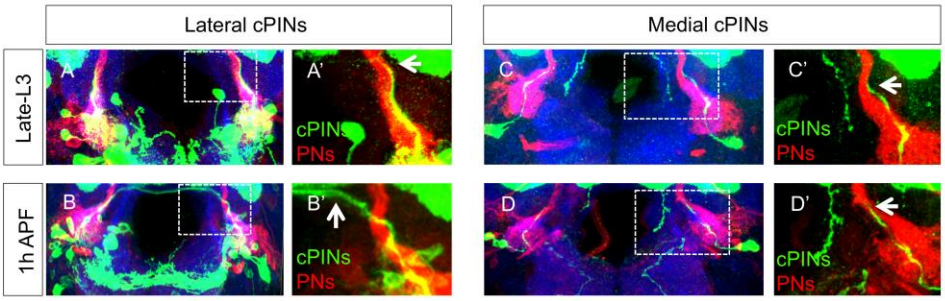

Supplementary Figure 7

Fig. S7. cPINs segregate from PNs in early AL development. (**A** and **C**) Innervation pattern of cPINs in larval and adult olfactory system. In late third instar larvae cPIN neurites of both lateral (A) and medial (C) classes start to innervate the developing AL (AL marked by the dendrites of PNs in red) and show extension (white arrow in A' and C') along the axonal bundle of PNs. (**B** and **D**) Sequential bilateral projection of cPIN classes. cPINs of lateral class start to project contralateral AL and commence antennal commissure formation by approximately 1h APF (B and white arrow in B'), whereas medial class lags behind and shows ipsilateral innervation at this given time (D, and white

arrow in D'). Genotypes: (A-B) *;UAS-mCD8::GFP; R12C01-Gal4/GH146-QF, QUAS-mtdTomato-3xHA* (C-D) *;UAS-mCD8::GFP; R20F11-Gal4/GH146-QF, QUAS-mtdTomato-3xHA.* Labeling: cPIN projections are labeled by Gal4 driven UAS-mCD8::GFP which were stained with anti-GFP (in green), dendrites and axons of PNs were visualized QF driven mtdTomato fluorescent protein and brain is counterstained with neuropil marker DN-cadherin (blue).

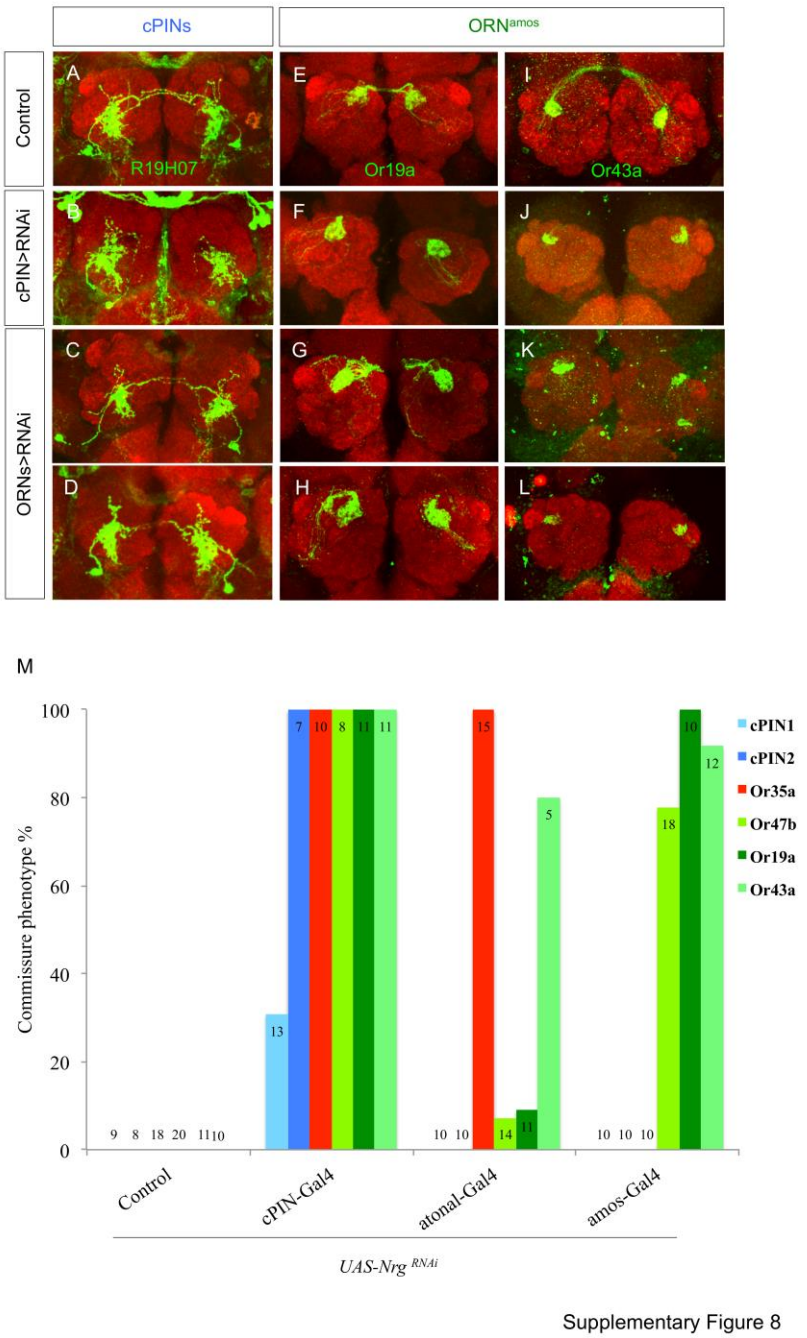

Supplementary Figure 8

Fig. S8. Cell autonomous and non-autonomous function of Neuroglian in cPINs and ORNs. Knock down of Nrg via targeted RNAi showed connectivity phenotype and revealed its cell-autonomous requirement in cPINs (compare **B** with **A**), whereas no effect on cPIN development can be detected following the removal of Nrg in ORNs (**C** and **D**). Like Or47b (see Fig. 4), cPIN specific removal of Nrg affects other *amos*-positive classes (Or19a in **F** and Or43a in **J**), which display a bilateral innervation in wild type (**E** and **I**). Removal of Nrg in pioneer ORNs via *atonal-Gal4* also showed cell non-autonomous effects on the *amos*-ORNs (**G** and **K**). *amos-Gal4* driven Nrg RNAi showed a strong cell

specific requirement of Nrg in follower ORN development (**H** and **L**). (**M**). Quantification of commissure phenotype of two cPIN classes (cPIN1- *R20F11-Gal4*, Fig.4 and cPIN2-*R19H07-Gal4*), one *atonal*-positive (Or35a, Fig. 4) and three *amos*-positive classes (Or47b from Fig. 4, Or19a and Or43a). Genotypes: For cPIN specific knockdown (B) ;UAS-*Nrg^{RNAi}/R19H07-LexA;13XLexAop2-mCD8::GFP/R19H07-Gal4 and* (F and J) ;*UAS Nrg^{RNAi}/Orxx-mCD8::GFP; R19H07-Gal4.* For pioneer ORN class specific knockdown (C) ;*UAS-Nrg^{RNAi}/R19H07-LexA;13XLexAop2-mCD8::GFP/atonal-Gal4*, (G and K) ;*UAS Nrg^{RNAi}/Orxx-mCD8::GFP; atonal-Gal4.* For follower ORN class specific knockdown (D) *pebbeled-Gal4; UAS-Nrg^{RNAi}/ R19H07-LexA;13XLexAop2-mCD8::GFP*, (H and L) ;*UAS-Nrg^{RNAi}/amos-Gal4; Orxx-mCD8::GFP.* Labeling: All neuronal axons are labeled by Or-mCD8::GFP reporter which were stained with anti-GFP (in green), counterstained with neuropil marker DN-cadherin (red).

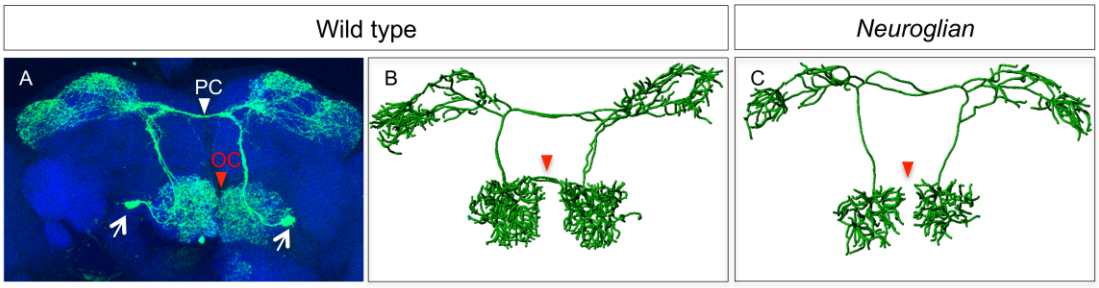

Supplementary Figure 9

Fig. S9. Neuroglian affects olfactory commissure development of CSD neurons. (**A**) Neuronal morphology of CSD (contralaterally-projecting Serotonin-immunoreactive Deutocerebral) neuron. Each AL of Drosophila is innervated ipsi-and contralaterally by a pair of CSDs (white arrow). The dendrites of CSD neuron innervate the ipsilateral AL, branches to the higher brain center on both hemisphere via protocerebral commissure (PC, white arrow head), innervate the contralateral AL and subsequently project back to the ipsilateral AL via olfactory commissure (OC, red arrow head). (**B**-**C**) The filament-tracing module of Imaris (Bitplane) reveals the 3-D organization of CSD neuron in wild type and

Nrg mutant. In wild type, both PC and OC are seen (B), whereas *Nrg* mutants show a specific loss of the OC (C). Genotypes: wild type: *nrg^{849}/+;UAS-mCD8::GFP;R37D04-Gal4*, *Nrg* mutant: *nrg^{849}/y;UAS-mCD8::GFP; R37D04-Gal4* Labeling: (A) Dendrites of CSD neurons are labeled with *R37D04-Gal4* driven *UAS-mCD8::GFP* (in green) stained with anti-GFP antibody and AL is counterstained with neuropil marker DN-cadherin (blue).

Table S1. Genotype of experiments.

1 A	*pebbled-Gal4 UAS-mCD8::GFP;;*
1 B	Canton S
1 C, C'	*A. aarabiensis*
1 D, D'	Canton S
1 E, E'	*nrg^{849} ;;*
1 F	*nrg^{849} /x; UAS-mCD8::GFP/Sg18.1-Gal4 ;*
1 G	*nrg^{849} /y; UAS-mCD8::GFP/Sg18.1-Gal4 ;*
1 H	*nrg^{849} /x;; R17H02-Gal4 UAS-mcherry*
1 I	*nrg^{849} /y;; R17H02-Gal4 UAS-mcherry*
1 J	*;hsmFL5; UAS-Flybow 1.1B/ R86G11-Gal4*
1 K	*nrg^{849} /y; hsmFL5; UAS-Flybow 1.1B, R86G11-Gal4*
1 L	*;+/Sg18.1-Gal4 ;Or47b-mCD8::GFP/+*
1 M	*;UAS-Nrg^{RNAi}/Sg18.1-Gal4 ;Or47b-mCD8::GFP/+*
1 N, N'	*nrg^{849} /x; UAS-Brp::GFP/Or47b-Gal4 ;*
1 O, O'	*nrg^{849} /y; UAS-Brp::GFP/Or47b-Gal4 ;*
1 P, P'	*;UAS-Nrg^{RNAi}; Or47b-mCD8::GFP /GH146-Gal4*
1 Q, Q'	*; UAS-Nrg^{RNAi}; Or47b-mCD8::GFP /+;OK107-Gal4*
1 R, R"	*; UAS-mCD8::GFP;;OK107-Gal4*
1 S-S"	*nrg^{849} /y; UAS-mCD8::GFP;;OK107-Gal4*

2 A, A', A"	*UAS-mCD8::GFP; UAS-mCD8::GFP;atonal-Gal4*
2 B, B', B"	*; UAS-mCD8::GFP;;OK107-Gal4*
2 C, C',C", C"'	*13XLexAop2-mCD8::GFP,10XUAS-mCD8::RFP;R20F11-LexA;R19H07Gal4*
2 D	*nrg^{849} /y; UAS-mCD8::GFP; R20F11-Gal4*
2 E	*nrg^{849} /y; UAS-mCD8::GFP; R19H07-Gal4*
2 F, F'	*hs-FLP;FRT42,UAS-mCD8::GFP/FRT42,Gal80; R19H07-Gal4*
2 G, G'	*UAS-mCD8::GFP; UAS-mCD8::GFP; R20F11-Gal4*
2 H, I, J	*UAS-mCD8::GFP; UAS-mCD8::GFP; R20F11-Gal4*
2 K, L, M	*nrg^{849} /y; UAS-mCD8::GFP; R20F11-Gal4*
2 N, O, P	*;UAS-mCD8::GFP; R20F11-Gal4/ GH146-QF, QUAS-mtdTomato-3xHA*

3 B-E	*nrg^{849} /x; UAS-mCD8::GFP; R86G11-Gal4*
3 F-I	*nrg^{849} /y; UAS-mCD8::GFP; R86G11-Gal4*
3 J-O	*;hsmFL5; UAS-Flybow 1.1B/ R86G11-Gal4*

3 R-T	*nrg^{849}/x; UAS-Brp::GFP/ R86G11-Gal4 ;*
3 S-U	*nrg^{849}/y; UAS-Brp::GFP/ R86G11-Gal4 ;*

4 B	*; R20F11-LexA/ CyO; 13XLexAop2-mCD8::GFP*
4 C	*;+/ CyO; atonal-Gal4/ Or35a-mCD8::GFP*
4 D	*; CyO/amos-Gal4; Or47b-mCD8::GFP*
4 E	*;UAS-Nrg^{RNAi}/R20F11-LexA;13XLexAop2-mCD8::GFP/R19H07-Gal4*
4 F	*;UAS-Nrg^{RNAi}; Or35a-mCD8::GFP; OK107-Gal4*
4 G	*;UAS-Nrg^{RNAi}; Or47b-mCD8::GFP; OK107-Gal4*
4 H	*;UAS-Nrg^{RNAi}/R20F11-LexA;13XLexAop2-mCD8::GFP/atonal-Gal4*
4 I	*;UAS-Nrg^{RNAi}; Or35a-mCD8::GFP; atonal-Gal4*
4 J	*;UAS-Nrg^{RNAi}; Or47b-mCD8::GFP; atonal-Gal4*
4 K	*pebbled-Gal4;Nrg^{RNAi}/R20F11-LexA;13XLexAop2-mCD8::GFP*
4 L	*;UAS-Nrg^{RNAi}/amos-Gal4; Or35a-mCD8::GFP*
4 M	*;UAS-Nrg^{RNAi}/amos-Gal4; Or47b-mCD8::GFP*
4 N	*nrg^{14}/y; P[nrg_wt]; R12C01-Gal4, UAS-mCD8::GFP*
4 N’	*nrg^{14}/y;P[nrg^{180}_ΔFIGQY];R12C01-Gal4, UAS-mCD8::GFP*
4 N”	*nrg^{14}/y; P[nrg^{180}_ΔC]; R12C01-Gal4, UAS-mCD8::GFP*
4 N”’	*nrg^{14}/y; P[nrg_ΔFERM]; R12C01-Gal4, UAS-mCD8::GFP*
4 O	*nrg^{14}/y; P[nrg_wt]/ UAS-mCD8::GFP; R19H07-Gal4*
4 O’	*nrg^{14}/y;P[nrg^{180}_ΔFIGQY]/ UAS-mCD8::GFP; R19H0 -Gal4*
4 O”	*nrg^{14}/y; P[nrg^{180}_ΔC]/ UAS-mCD8::GFP; R19H07-Gal4*
4 O”’	*nrg^{14}/y; P[nrg_ΔFERM/ UAS-mCD8::GFP; R19H0 -Gal4*
4 P	*nrg^{14}/y; P[nrg_wt]/ UAS-mCD8::GFP; Ir41a-Gal4*
4 P’	*nrg^{14}/y; P[nrg^{180}_ΔFIGQY]/ UAS-mCD8::GFP; Ir41a-Gal4*
4 P”	*nrg^{14}/y; P[nrg^{180}_ΔC]/ UAS-mCD8::GFP; Ir41a-Gal4*
4 P”’	*nrg^{14}/y; P[nrg_ΔFERM/ UAS-mCD8::GFP; Ir41a-Gal4*
4 Q	*nrg^{14}/y; P[nrg_wt]; Or47b-Gal4, UAS-mCD8::GFP*
4 Q’	*nrg^{14}/y; P[nrg^{180}_ΔFIGQY]; Or47b-Gal4, UAS-mCD8::GFP*
4 Q”	*nrg^{14}/y; P[nrg^{180}_ΔC]; Or47b-Gal4, UAS-mCD8::GFP*
4 Q”’	*nrg^{14}/y; P[nrg_ΔFERM]; Or47b-Gal4, UAS-mCD8::GFP*